

New Degrees of Freedom for High Performance Silicon Modulator Design

Xinbai Li, Fenghe Yang, Tiantian Li, Qingzhong Deng, Ruobing Chen, Zhiping Zhou*
State Key Laboratory of Advanced Optical Communication Systems and Networks
School of Electronics Engineering and Computer Science, Peking University, Beijing, 100871, China
*zjzhou@pku.edu.cn

Abstract—This paper introduces oblique and lateral components into interleaved junction. Analytical model to characterize the complex interleaved interfaces is proposed, achieving nearly 23% reduction on energy consumption and 50% on $V_{\pi}L_{\pi}$ compared with traditional lateral junctions.

I. INTRODUCTION

Interleaved junctions can achieve better modulation efficiency ($V_{\pi}L_{\pi}$) than lateral junctions, and therefore play a pivotal role in reducing phase shifter length and insertion loss. Recently reported interleaved junctions have realized $V_{\pi}L_{\pi}$ as low as 0.6~1 V·cm with 200 nm pitch [1-3]. However, the inefficient light-carrier overlap induces greater capacitance that in turn results in higher energy consumption [2, 3]. In this paper, oblique and lateral contribution is introduced as two additional degrees of freedom in high performance interleaved junctions and an analytical model is proposed for accurate characterization. This work provides a practical solution for simultaneously optimizable $V_{\pi}L_{\pi}$ and energy consumption, which remained elusive for conventional lateral and interleaved junctions.

II. ANALYTICAL MODEL

To characterize the proposed junction performance (Fig. 1(a)), 3D simulation is usually required to account for the heterogeneity along the propagation direction. However, the needed absolute error of Δn_{eff} (per unit length) $\sim 10^{-6}$ is improbable to obtain. To address this problem, this work puts forward an analytical model to yield accurate Δn_{eff} with 2D obtainable quantities: horizontal junction contribution Δn_h (Fig.1 (b)) and lateral junction contribution Δn_l (Fig.1 (c)). 2D simulation validity is verified by comparing with two papers of basic junction modeling that provide simulation and experimental consolidation [1, 4]. Because junction depletion area ($\Delta n \sim 10^{-3}$) only exerts perturbation on the mode profile, the effect of oblique junction interfaces can be differentiated to horizontal and lateral contribution (Fig. 1(a)). Total effective index change per unit length can be given by Eq. (1), where L_{min} is the minimum doping size, α is the oblique angle and Δw is the width change of depletion region. As α approaches zero, the equation form converges to conventional interleaved junction as expected. Equation (1) discriminates the contribution from four junction components, numerically shown in Fig. 1 (d-e). Two influences exerted by oblique angle can be observed: a)

adjusting the Δn_{eff} contribution proportion from four different junction components; b) prolonging interleaved junction interface and thus lateral contribution, as well as PN pitch length (210 nm) by $1/\cos\alpha$. When lateral contribution increment is more than the extension of pitch length, modulation effect benefits from obliqueness.

III. RESULTS

Uniform doping is adopted here to provide physical perceptions. With proper layout correction, Gaussian doping profile will show the same trend as uniform doping [3]. Hence, uniform doping gives physically instructive understandings. Numerical visualization of Eq. (1) is shown in Fig. 2 and the optimal results are marked. Full-swing energy consumption is analyzed here, since this is a parameter that does not change with driving conditions and solely reflects PN junction electro-optic capabilities. Energy reaches minimum at $\text{offset} < 225$ nm (smaller than waveguide width) where light-carrier overlap is more efficient, as opposed to the conventional interleaved junctions where $\text{offset} = 225$ nm always consume the least energy. [α, offset]=[0,0] represents conventional lateral junction in waveguide center, exhibiting [1.02 V·cm, 4.97 pJ/bit]. In comparison, oblique junction can achieve [0.44 V·cm, 4.43 pJ/bit] at 30.3° for lowest $V_{\pi}L_{\pi}$, and [0.51 V·cm, 3.84 pJ/bit] at 32.1° for lowest energy. The trade-off is no longer significant due to improved light-carrier overlap. Energy consumption and $V_{\pi}L_{\pi}$ are reduced by 23% and 50% respectively compared with conventional lateral junctions, which is quite considerable among modulator PN junction studies. Design rules are also taken into consideration (see Fig. 2 caption) to ensure feasibility. It indicates that the best modulation efficiency can be well realized, and a nearby set of structural parameters for best energy is within reach.

IV. CONCLUSIONS

Two new degrees of freedom, oblique and lateral components, are introduced to the interleaved junction. An analytical model is proposed for the characterization, showing nearly 23% and 50% performance enhancement on both modulation efficiency and energy consumption. The underlying physical concept is that the two additional design dimensions prolong junction interface and enhance light-carrier overlap. This work also shows that modulation efficiency and energy consumption can be simultaneously enhanced, as opposed to the case of conventional lateral and interleaved

junction. The proposed design is highly favorable in applications such as optical communications and interconnects.

$$\begin{aligned} \Delta n_{eff} = & \frac{\cos \alpha}{2L_{min}} (\Delta n_h (offset + L_{min} \sin \alpha / 2) \Delta w + \Delta n_h (|offset - L_{min} \sin \alpha / 2|) \Delta w) \\ & + \frac{\cos \alpha}{2L_{min}} \left(\tan \alpha \int_{-offset - L_{min} \sin \alpha / 2}^{offset + L_{min} \sin \alpha / 2} \Delta n_l(x) dx + \tan \alpha \int_{-offset + L_{min} \sin \alpha / 2}^{offset - L_{min} \sin \alpha / 2} \Delta n_l(x) dx \right) \\ & + \frac{\cos \alpha}{2L_{min}} \left(\cot \alpha \int_{-offset - L_{min} \sin \alpha / 2}^{offset + L_{min} \sin \alpha / 2} \Delta n_l(x) dx + \cot \alpha \int_{-offset + L_{min} \sin \alpha / 2}^{offset - L_{min} \sin \alpha / 2} \Delta n_l(x) dx + f_h(offset) \Delta w \right) \end{aligned} \quad (1)$$

$$f_h(offset) = \begin{cases} \Delta n_h(offset + L_{min} \sin \alpha / 2) - \Delta n_h(offset - L_{min} \sin \alpha / 2), & offset - L_{min} \sin \alpha / 2 > 0 \\ \Delta n_h(offset + L_{min} \sin \alpha / 2) + \Delta n_h(-offset - L_{min} \sin \alpha / 2), & offset - L_{min} \sin \alpha / 2 \leq 0 \end{cases}$$

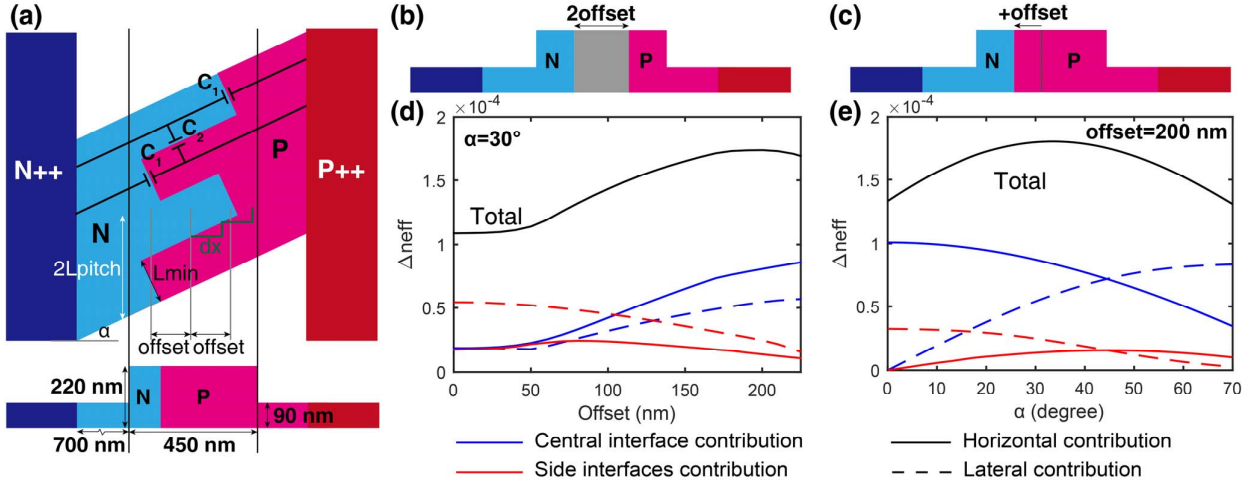


Fig. 1. (a) Schematic of oblique junction, top-view and cross-sectional view. (b) Illustration of 2D simulation of Δn_h and (c) Δn_l . (d) Relations between Δn_{eff} and $offset$, at fixed $\alpha=30^\circ$. (e) Relations between Δn_{eff} and α , at fixed $offset=200$ nm. Doping parameters are $5 \times 10^{17}/\text{cm}^3$ and $1 \times 10^{18}/\text{cm}^3$ for P and N doping, $10^{20}/\text{cm}^3$ for heavy doping.

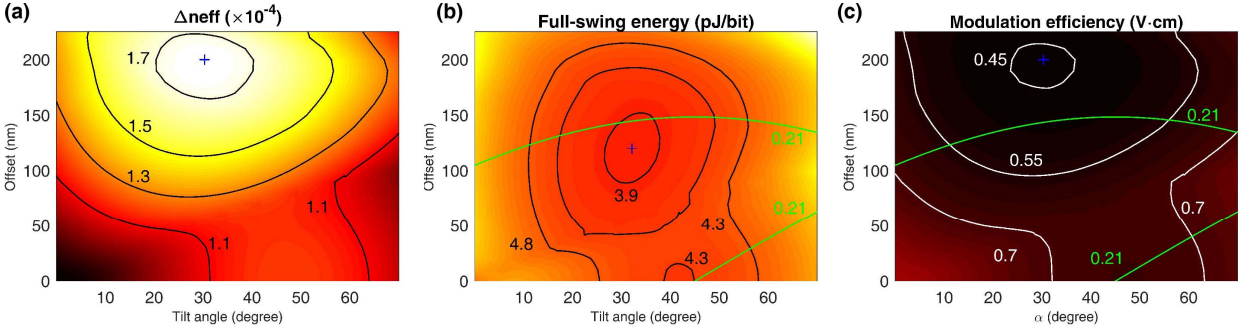


Fig. 2. Analysis of (a) Δn_{eff} , (b) energy consumption and (c) modulation efficiency. Energy calculation assumes 1-mm long phase shifter and push-pull modulation of full transmission swing (0-100%). The green lines in (b) show the design rule of feature size: $|2offset - L_{min} \sin \alpha| \geq L_{min}$. The regions outside of the two green lines do not violate design rule. Extrema are shown in figures by "+" marker where the values are: (a) $[\alpha, offset, \Delta n_{eff}] = [30.3^\circ, 200 \text{ nm}, 0.00017]$ (b) $[\alpha, offset, \text{Energy}] = [32.1^\circ, 120 \text{ nm}, 3.84 \text{ pJ/bit}]$ (c) $[\alpha, offset, V_{\pi} L_{\pi}] = [30.3^\circ, 200 \text{ nm}, 0.44 \text{ V}\cdot\text{cm}]$. $L_{min}=210$ nm is chosen to match CMOS 90 nm node design rules.

This work was partially supported by the Major International Cooperation and Exchange Program of the National Natural Science Foundation of China under Grant 61120106012.

REFERENCES

[1] X. Xiao, H. Xu, X. Li, Y. Hu, K. Xiong, Z. Li, T. Chu, Y. Yu, and J. Yu, "25 Gbit/s silicon microring modulator based on misalignment-tolerant

interleaved PN junctions," Opt Express, vol. 20, pp. 2507-15, 2012-01-30 2012.

[2] I. Goykhman, et al., "Optics Express, vol. 21, p. 19518, 2013-08-26 2013.

[3] H. Yu, et al., "Doping Geometries for 40G Carrier-Depletion-Based Silicon Optical Modulators," in Optical Fiber Communication Conference (OFC), Los Angeles, California, 2012, p. OW4F.4.

[4] R. Dube-Demers, et al., "Analytical Modeling of Silicon Microring and Microdisk Modulators With Electrical and Optical Dynamics," Journal of Lightwave Technology, vol. 33, pp. 4240-4252, 2015.